Article

Theoretical Study of the Conversion of Sulfonyl Precursors into Chains of Poly(*p*-phenylene vinylene)

L. Claes, J.-P. Franois, and M. S. Deleuze

J. Am. Chem. Soc., **2003**, 125 (23), 7129-7138• DOI: 10.1021/ja021295e • Publication Date (Web): 15 May 2003

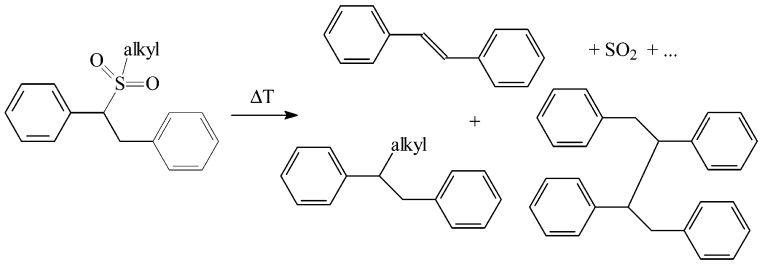

More About This Article

Additional resources and features associated with this article are available within the HTML version:

- Supporting Information
- Links to the 4 articles that cite this article, as of the time of this article download
- Access to high resolution figures
- Links to articles and content related to this article
- Copyright permission to reproduce figures and/or text from this article

View the Full Text HTML

J|A|C|S
ARTICLES
Published on Web 05/15/2003

Theoretical Study of the Conversion of Sulfonyl Precursors into Chains of Poly(*p*-phenylene vinylene)

L. Claes, J.-P. François, and M. S. Deleuze*

Contribution from the Institute for Materials Science (IMO), Department SBG, Limburgs Universitair Centrum, Universitaire Campus, B-3590 Diepenbeek, Belgium

Received October 22, 2002; Revised Manuscript Received February 20, 2003; E-mail: michael.deleuze@luc.ac.be

Abstract: The elimination and side reactions involved in the thermal conversion of sulfonyl precursor chains into poly(*p*-phenylene vinylene) (PPV) have been studied in detail, using Density Functional theory, along with the MPW1K functional. The performance of the MPW1K functional for describing radical dissociation and internal conversion reactions of sulfonyl precursors has been assessed against the results of benchmark CCSD(T) calculations. Enthalpies as well as entropies are calculated at different temperatures at the level of the rigid rotor−harmonic oscillator approximation. Entropy effects on internal elimination reactions are very limited. In sharp contrast, at the temperatures under which the conversion is usually performed (550 K), entropy contributions to the activation energies are found to be very significant and to strongly favor direct radical dissociations of the precursors. Further radical side reactions following an E_i conversion through an alkyl substituent may also significantly contribute to the formation of sp^3 defects and/or cross-linked structures in the polymer—an advantageous feature for the making of materials with improved photoluminescence efficiencies.

1. Introduction

Poly(*p*-phenylene vinylene) (PPV) is a polymer with attractive properties such as a high electrical conductivity,[1] electroluminescence,[2] photoluminescence,[3] and photoconductivity.[4] Applications such as battery electrodes, capacitor electrolytes, electrostatic discharge coatings, and solar cells,[5−11] are now at hand. Because PPV is insoluble, it can be directly processed only with great difficulty. One approach to circumvent this problem is the use of a precursor route in which a nonconjugated soluble precursor of the polymer is first mechanically treated and thereafter converted thermally into PPV.[12−15]

Depending on which precursor is used, different molecular architectures or morphologies are obtained. The morphology of the final polymer may have a large effect on the performance of the material in the specific application.[14] At present, several precursors enable the making of PPV samples with the desired properties for applications in electronic devices. It has been in particular recently observed that PPV can be formed from a sulfonyl-based precursor. The obtained polymer exhibits photoluminescence efficiencies as high as 12%.[16]

UV−vis techniques indicate a smaller conjugation length for the polymer obtained by elimination of the sulfonyl precursor compared to the sulfoxide precursor, a feature that can be attributed to sp^3 defects. The first absorption band ($\lambda_{max} = 375$ nm) of the polymer derived from the sulfonyl precursor is found to be blue-shifted in comparison with the polymer derived from the sulfoxide precursor ($\lambda_{max} = 416$ nm).[16] Also, the polymer derived from the sulfonyl precursor exhibits a fine structure in the UV absorption spectrum, due to various vibrational levels associated with the shorter conjugated units. No visible sulfonyl signal remains in the IR spectrum after elimination, indicating that the shorter conjugation length is not due to incomplete elimination. However, alkyl signals are present, which are thought to originate from alkyl side groups on the polymer backbone or from cross-linked structures. The products formed upon elimination and degradation of the sulfonyl precursor have

(1) Muras, I.; Ohnishi, T.; Noguchi, T.; Hirooka, M. *Synth. Met*. **1987**, *17*, 639.
(2) Pichler, K. *Philos. Trans. R. Soc. London, Ser. A* **1997**, *355*, 829.
(3) Burroughes, J. H.; Bradley, D. D. C.; Brown, A. R.; Marks, R. N.; Mackay, K. D.; Friend, R. H.; Burn, P. L.; Holmes A. B. *Nature* **1990**, *347*, 539.
(4) Antoniadis, H.; Hsieh, B. R.; Abkowitz, M. A.; Jenekhe, S. A.; Stolka, M. *Synth. Met*. **1994**, *62*, 265
(5) Pei, Q.; Yu, G.; Zhang, C.; Yang, Y.; Heeger, A. J. *Science* **1995**, *269*, 1086.
(6) Pei, Q.; Yu, G.; Zhang, C.; Yang, Y.; Heeger, A. J. *J. Am. Chem. Soc.* **1996**, *118*, 3922.
(7) Sirringhaus, H.; Tessler, N.; Friend, R. H. *Science* **1998**, *280*, 1741.
(8) Ganstrom, M.; Arias, A. C.; Lux; Anderson, M. R.; Friend, R. H. *Nature* **1998**, *395*, 257.
(9) Tessler, N.; Denton, G. J.; Friend, R. H. *Nature* **1995**, *382*, 695.
(10) Hide, F.; Diaz-Garzia, M. A.; Schwartz, B. J.; Anderson, M. R.; Pei, Q.; Heeger, A. J. *Science* **1996**, *273*, 1833.
(11) Tessler, N. *Adv. Mater*. **1999**, *11*, 363.
(12) (a) Louwet, F.; Vanderzande, D.; Gelan, J. *Synth. Met*. **1992**, *52*, 125. (b) Louwet, F.; Vanderzande, D. J.; Gelan, J. M.; Mullens, J. *Macromolecules* **1995**, *28*, 1330. (c) Louwet, F.; Vanderzande, D.; Gelan, J. *Synth. Met*. **1995**, *69*, 509. (d) Vanderzande, D. J.; Issaris, A. C.; Van Der Borght, M. J.; van Breemen, A. J. J. M.; de Kok, M. M.; Gelan, J. M. *Macromol. Symp*. **1997**, *125*, 189. (e) Vanderzande, D. J.; Issaris, A. C.; Van Der Borght, M. J.; van Breemen, A. J. J. M.; de Kok, M. M.; Gelan, J. M. *Polym. Prepr*. **1997**, *38*, 321. (f) de Kok, M. M.; van Breemen, A. J. J. M.; Carleer, R. A. A.; Adriaensens, P. J.; Gelan, J. M.; Vanderzande, D. J. *Acta Polym*. **1999**, *50*, 28. (g) Kesters, E.; Lutsen, L.; Vanderzande, D.; Gelan, J. *Synth. Met*. **2001**, *119*, 311.
(13) de Kok, M. M. Chemical modification of sulfoxide precursor polymers towards PPV. Ph.D. Thesis, Limburgs Universitair Centrum, Belgium, 1999.
(14) Son, S.; Dodabalapur, A.; Lovinger, A. J.; Galvin, M. E. *Science* **1995**, *269*, 376.
(15) Wessling, R. A.; Zimmerman, R. G. U.S. Patent 3,401,152, 1968.
(16) Kesters, E.; de Kok, M. M.; Carleer, R. A. A.; Czech, J. H. P. B.; Adriaensens, P. J.; Gelan, J. M.; Vanderzande, D. J. *Polymer* **2002**, *43*, 5749.

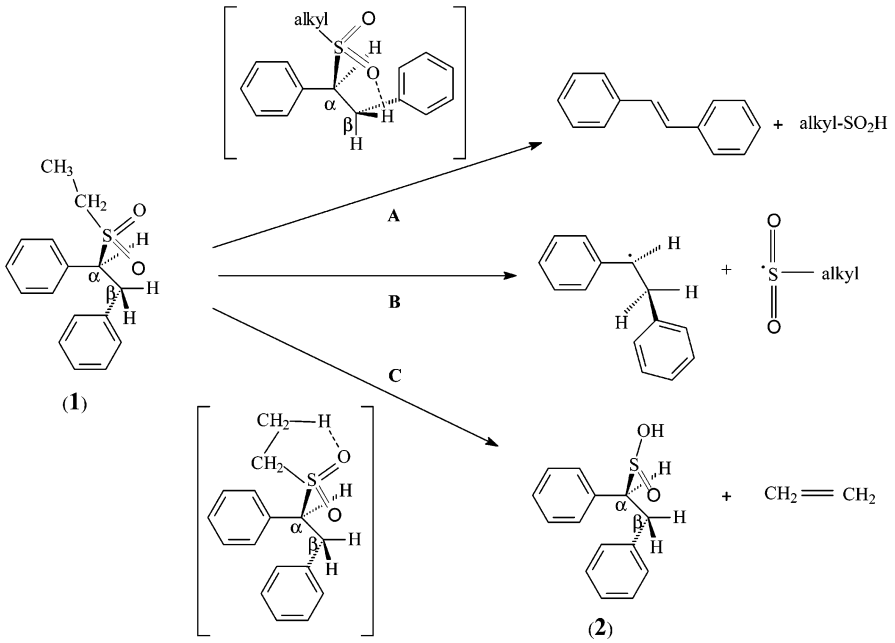

Figure 1. E_i reaction mechanism via the polymer backbone (A), the radical elimination mechanism (B), and a mixed pathway, starting with an E_i reaction via the alkyl chain (C).

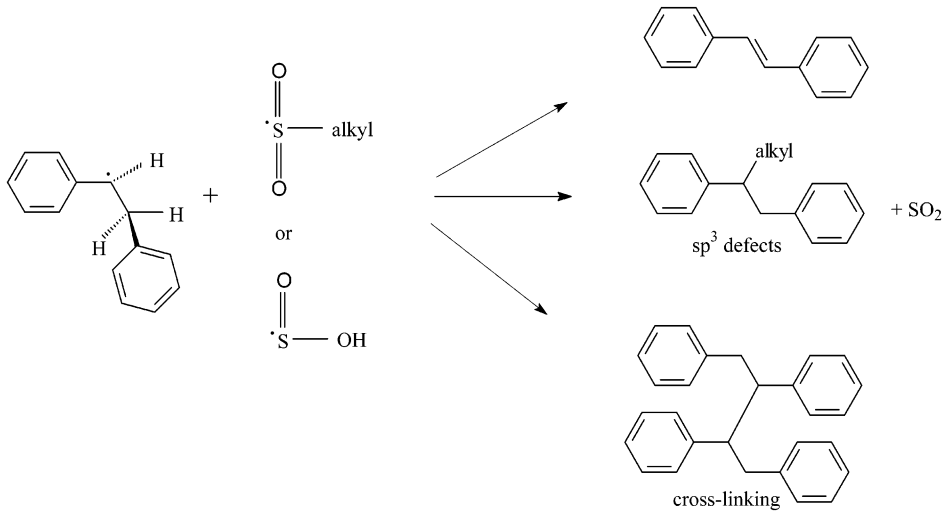

Figure 2. Formation of structural defects as a consequence of mechanism B in Figure 1 or of mechanism E in Figure 3.

been followed with flash pyrolysis gas chromatography−mass spectroscopy (GC−MS). Octane and octene were clearly detected in the analysis.

Certainly, the presence of these structural defects must adversely affect the conductive properties of the polymer through a limitation of the average π-conjugation length and, thus, the mobility of the charge carriers, whereas optical properties of the material such as the photoluminescence efficiency are improved by the larger separation of chains.[17] Via which mechanism the sulfonyl precursor eliminates is still an unresolved issue. Two primary processes can be operative. One possibility is a concerted internal elimination (E_i) mechanism[18] (paths A and C in Figure 1), as proposed by Cubbage et al. for closely related sulfone species.[19] The E_i reaction is a single-step process in which the sulfonyl functionality acts simultaneously as a leaving group and as a proton abstracting group. This reaction is therefore characterized by a cyclic transition structure. A second possibility is a radical mechanism implying a homolytic breakage of the C_α−S bond (path B in Figure 1), inducing in turn the homolytic breakage of the nearby C_β−H bond and the formation of a double bond. Alternatively, the homolytic breakage of the C_α−S bond can be followed by SO_2 elimination. In that way, an alkyl radical is formed, which can lead to branched or cross-linked polymer chains (Figure 2).

To the best of our knowledge, theoretical studies of E_i reactions of sulfone compounds are limited to the calculation of activation enthalphies, including corrections for zero-point energies, at the MP2/6-311+G(3df,2p)//MP2/6-31G(d,p) level.[19] On the other hand, the E_i reactions of several sulfoxide precursors have already been extensively studied on various theoretical

(17) Yan, M.; Rothberg, L. J.; Papadimitrakopoulos, F.; Galvin, M. E.; Miller, T. M. *Phys. Rev. Lett.* **1994**, *73*, 744.
(18) Hurd, C. D.; Blunck, F. H. *J. Am. Chem. Soc.* **1938**, *60*, 2419.
(19) Cubbage, J. W.; Vos, B. W.; Jenks, W. S. *J. Am. Chem. Soc.* **2000**, *122*, 4968.

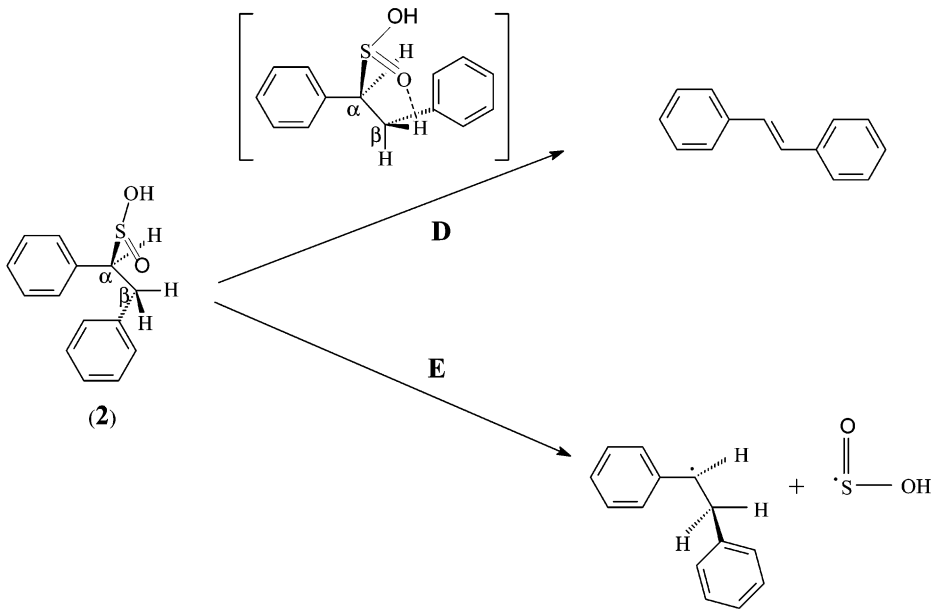

Figure 3. E_i reaction mechanism (D) and the radical elimination mechanism (E) of intermediate **2**.

grounds.[20,21] The interested reader is referred in particular to a thorough theoretical study[21] of the conversion of sulfoxide precursors into model oligomers of conjugated polymers (PPV, PITN), using a new hybrid Density Functional, namely, the so-called Modified Perdew−Wang one-parameter model for kinetics (MPW1K). This functional has been specifically designed[22,23] for accurate but tractable computations of barrier heights and saddle point geometries. In this hybrid functional, the proportion of Hartree−Fock exchange has been significantly increased compared with the more traditional B3LYP (Becke three-parameter Lee−Yang−Parr),[24,25] mPW1PW91 (modified Perdew−Wang Perdew−Wang−1991),[26] etc., approximations, enabling a better description of nonlocal electron interactions in transition states. The performance of this Density Functional approach has been specifically assessed for the internal elimination reaction of sulfoxide precursors by comparison against available experimental activation energies and benchmark CCSD(T) calculations (Coupled Cluster theory with single and double excitations supplemented with a quasi-perturbative estimate of the effect of triple excitations[27,28]).[21] In the present study, the reliability of the MPW1K functional in describing internal elimination and radical bond dissociations of sulfonyl precursors will be verified in the same way.

The main purpose of the present work is to investigate on reliable theoretical grounds the origin of sp^3 defects inherent to the synthesis of poly(*p*-phenylene vinylene) via the sulfonyl precursor route, an issue of obvious relevance for the design of polymer materials and devices with well-defined electro-optical properties. The present contribution reconsiders the MPW1K functional for studying possible reaction mechanisms in the conversion of the sulfonyl precursor of stilbene, the smallest oligomer approaching the structure of PPV. Specifically, internal elimination reactions (paths A and C in Figure 1 and path D in Figure 3) and competitive radical dissociation pathways (path B in Figure 1 and path E in Figure 3) will be investigated. As will be shown, upon taking into account significant changes in the entropy, direct radical dissociations provide a qualitative but satisfactory explanation for the observed sp^3 defects[16] in the obtained material. One minor difference with experiment relates to the fact that experimentally *n*-octylsulfonyl precursors were converted, whereas the calculations presented in this work have been made for an ethylsulfonyl precursor, for the sake of tractability. With regard to the proposed mechanisms, it is unlikely that slightly enhanced steric hindrances with larger but highly flexible alkyl chains in the *n*-octylsulfonyl precursors will result in a qualitatively significant difference.

The performance of the MPW1K functional will be preliminarily assessed for radical dissociations and E_i conversions of small sulfone compounds by comparison against a series of HF (Hartree−Fock), MP2 (second-order Møller−Plesset), MP4(SDQ) (fourth-order Møller−Plesset including single, double, and quadruple substitutions), and benchmark CCSD(T) calculations in conjunction with basis sets of improving quality. The E_i conversion of the sulfonyl precursor of ethylene (Figure 4) and the radical dissociation reaction of dimethylsulfonyl (Figure 5) have been considered as model test cases.

2. Methodological Details

The transition states (TS) of the investigated E_i reactions have been located by the reaction coordinate method, also referred to as the STQN method (transition state optimizations using synchronous transit-guided quasi-Newton method).[29] The nature of the stationary points identified on the reaction pathway has been easily verified through vibrational analysis. All ab initio calculations described in this work have been carried out using the Gaussian98 package of programs.[30] The geometries

(20) Cubbage, J. W.; Guo, Y.; McCulla, R. D.; Jenks, W. S. *J. Org. Chem.* **2001**, *66*, 8722.
(21) Claes, L.; François, J. P.; Deleuze, M. S. *J. Am. Chem. Soc.* **2002**, *124*, 7563.
(22) Lynch, B. J.; Fast, P. L.; Harris, M.; Truhlar, D. G. *J. Phys. Chem. A* **2000**, *104*, 4811.
(23) Lynch, B. J.; Truhlar, D. G. *J. Phys. Chem. A* **2001**, *105*, 2936.
(24) Becke, A. D. *J. Chem. Phys.* **1993**, *1372*, 98, 5648.
(25) Lee, C.; Yang, W.; Parr, R. G. *Phys. Rev. B* **1988**, *37*, 785.
(26) Adamo, C.; Barone, V. *J. Chem. Phys.* **1998**, *108*, 664.
(27) Purvis, G. D.; Bartlett, R. J. *J. Chem. Phys.* **1982**, *76*, 1910.
(28) Raghavachari, K.; Trucks, G. W.; Pople, J. A.; Head-Gordon, M. *Chem. Phys. Lett.* **1989**, *157*, 479.
(29) (a) Peng, C.; Ayala, P. Y.; Schlegel, H. B.; Frisch, M. J. *J. Comput. Chem.* **1996**, *17*, 49. (b) Peng, C.; Schlegel, H. B. *Israel J. Chem.* **1994**, *33*, 449.

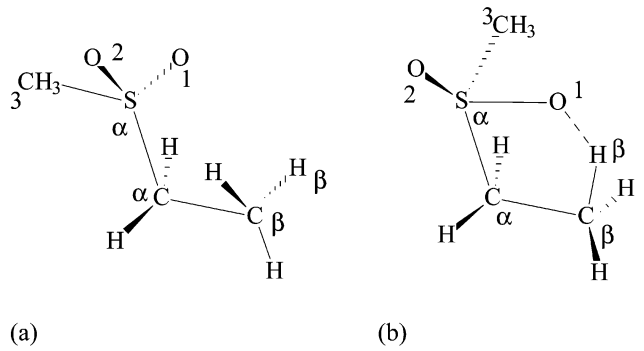

Figure 4. Molecular structure of the reactant (a) and of the transition state (b) of the sulfonyl precursor leading to ethylene through internal elimination.

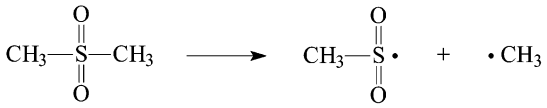

Figure 5. Homolytical dissociation of the $C_\alpha-S$ bond in dimethylsulfonyl.

of the precursor, transition state, and products involved in the reactions sketched in Figures 1−3 have been fully optimized with tight convergence criteria at the MPW1K level using the 6-311G** basis. In this work, as in ref 21, activation barriers or reaction energies reported as $\Delta U^{\ddagger}$ or ΔU values are simply obtained as differences of total electronic energies.

Activation enthalpies ($\Delta H^{\ddagger}$), as well as activation entropies ($\Delta S^{\ddagger}$) and Gibbs free activation energies ($\Delta G^{\ddagger}$), have been further computed at temperatures ranging from 300 to 600 K from canonical partition functions obtained for an ideal polyatomic gas under a pressure of 1 atm, using the standard RRHO (rigid rotor harmonic oscillator) model and Boltzmann statistics (see refs 31 and 32 or any textbook of molecular statistical mechanics). The computed enthalpies therefore incorporate zero-point vibrational energies, PV-work terms, and thermodynamical corrections. The interested reader is referred in particular to Chapter 8 of ref 31 for a review of the canonical rotational and vibrational partition functions implemented in the Gaussian package of programs, and references therein for practical thermodynamical calculations on polyatomic molecules. Finally, the charge transfers and rearrangements of the electron density occurring during the E_i conversion of the sulfonyl precursor of *trans*-stilbene are discussed on the basis of Mulliken[33,34] and Natural Population Analyses[34] (NPA) of the computed MPW1K/6-311G** electron densities.

The dependence of the structural results and energies on the quality of the basis set and on the amount of electron correlation included in the computations has been carefully assessed for the particular case of the E_i reaction toward ethylene, in a preliminary calibration step. The geometries of the reactant and transition state (Figure 4) have been fully optimized at the MP2 and DFT(MPW1K) levels, using a series of basis sets of improving quality. The basis sets that have been considered are the standard 6-31G**,[35,36] 6-311G**,[37] and 6-311++G**,[38] bases, as well as Dunning's correlation consistent basis sets (cc-pVXZ),[39] of double (X = D) and triple (X = T) zeta quality. To assess the quality of the MPW1K method against benchmark theories, the corresponding E_i activation energy is also compared with the results of single-point CCSD(T) calculations, with basis sets of increasing size, on the MP2/6-311++G** ground state and transition state geometries. Similarly, the reliability of the MPW1K functional in determining radical bond dissociation energies has been verified by single-point calculations on the reactants and products of the radical dissociation reaction of dimethylsulfonyl (Figure 5), at the MP2, MP3, MP4(SDQ), CCSD, and CCSD(T) levels, using basis sets of increasing size. These single-point calculations have been performed on MP2/cc-pVTZ optimized structures.

3. Calibration of the MPW1K Functional

3.1. E_i Elimination of the Sulfonyl Precursor of Ethylene. To test the performance of the MPW1K functional and the effect of the size of the basis set, the E_i reaction leading to ethylene has been first considered. The main structural features computed for the sulfonyl precursor of ethylene and the related transition state are plotted in panels a and b of Figure 4 and compiled in Tables 1 and 2 for different basis sets at the MPW1K and MP2 levels, respectively. As is immediately apparent from Table 1, convergence of the MPW1K geometries is seen among basis sets such as 6-31G**, 6-311G**, 6-311++G**, and cc-pVTZ. Compared with these, the double-ζ correlation consistent cc-pVDZ basis set leads to systematically longer $S-O_1$ and $S-O_2$ bond lengths for both the reactant and transition state geometries. The same feature is observed at the MP2 level (Table 2).

The transition state (Figure 4b) is a practically planar five-membered ring, which is consistent with the model of an E_i reaction. During the conversion, the H_β atom is transferred from the C_β atom to one of the O atoms, with a $C_\beta-H_\beta-O$ bond angle of ∼156°. The $C_\alpha-C_\beta$ bond length decreases by ∼0.123 Å from the precursor to the transition state.

The MP2 geometries (Table 2) nicely match those obtained by means of the MPW1K functional (Table 1). The computed bond angles and dihedral angles are overall practically the same at both levels. The largest discrepancies between the two methods are observed for the bond lengths characterizing the leaving group, that is, the $C_\alpha-S$, $S-O_1$, $S-O_2$, and $S-C_3$ bond lengths. The MPW1K bond lengths pertaining to the $S-O_1$, $S-O_2$, and $S-C_3$ bond lengths are systematically slightly shorter by ∼0.01−0.025 Å than those obtained with the MP2 method. In comparison with the MP2 result, the $C_\alpha-S$ bond length is slightly too large, by ∼0.020 Å, at the MPW1K level in the transition state, and slightly too short, by ∼0.01 Å, in the reactant state. On the other hand, at the MPW1K level, the O_1-H_β bond distance in the transition state is a little too short, by ∼0.01−0.02 Å, whereas this bond is found to be slightly

(30) Frisch, M. J.; Trucks, G. W.; Schlegel, H. B.; Scuseria, G. E.; Robb, M. A.; Cheeseman, J. R.; Zakrzewski, V. G.; Montgomery, J. A., Jr.; Stratmann, R. E.; Burant, J. C.; Dapprich, S.; Millam, J. M.; Daniels, A. D.; Kudin, K. N.; Strain, M. C.; Farkas, O.; Tomasi, J.; Barone, V.; Cossi, M.; Cammi, R.; Mennucci, B.; Pomelli, C.; Adamo, C.; Clifford, S.; Ochterski, J.; Petersson, G. A.; Ayala, P. Y.; Cui, Q.; Morokuma, K.; Malick, D. K.; Rabuck, A. D.; Raghavachari, K.; Foresman, J. B.; Cioslowski, J.; Ortiz, J. V.; Stefanov, B. B.; Liu, G.; Liashenko, A.; Piskorz, P.; Komaromi, I.; Gomperts, R.; Martin, R. L.; Fox, D. J.; Keith, T.; Al-Laham, M. A.; Peng, C. Y.; Nanayakkara, A.; Gonzalez, C.; Challacombe, M.; Gill, P. M. W.; Johnson, B. G.; Chen, W.; Wong, M. W.; Andres, J. L.; Gonzalez, C.; Head-Gordon, M.; Replogle, E. S.; Pople, J. A. *Gaussian 98*, revision A.7; Gaussian, Inc.: Pittsburgh, PA, 1998.
(31) McQuarrie, D. A. *Statistical Mechanics*; Harper and Row: New York, 1976.
(32) Herzberg, G. H. *Molecular Spectra and Molecular Structure. II Infrared and Raman Spectra of Polyatomic Molecules*; Van Nostrand Reinhold: New York, 1945.
(33) Szabo, A.; Ostlund, N. S. *Modern Quantum Chemistry*; McGraw-Hill Publishing: New York, 1982.
(34) (a) Reed, A. E.; Weinstock, R. B.; Weinhold, F. *J. Chem. Phys.* **1985**, *83*, 735. Natural Population Analysis. (b) Lipkowitz, K. B.; Boyd, D. B. Population analysis and electron densities from quantum mechanics. In *Reviews in Computational Chemistry*; Bachrach, S. A., Ed.; VCH Publisher: 1994; p 171 and references therein.
(35) Francl, M. M.; Pietro, W. J.; Hehre, W. J.; Binkley, J. S.; Gordon, M. S.; DeFrees, D. J.; Pople, J. A. *J. Chem. Phys.* **1982**, *77*, 3654.
(36) Hariharan, P. C.; Pople, J, A. *Chem. Phys. Lett.* **1972**, *66*, 217.
(37) (a) Krishnan, R.; Binkley, J. S.; Seeger, R.; Pople, J. A. *J. Chem. Phys.* **1980**, *72*, 650. (b) McLean, A. D.; Chandler, G. S. *J. Chem. Phys.* **1980**, *72*, 5639.
(38) Frisch, M. J.; Pople, J. A.; Binkley, J. S. *J. Chem. Phys.* **1984**, *60*, 3265.
(39) Dunning, T. H., Jr. *J. Chem. Phys.* **1989**, *90*, 1007.

Table 1. Main Geometrical Characteristics of the Sulfonyl Precursor (pre) and Transition State (TS) of Ethylene (MPW1K Results)[a]

	6-31G**		6-311G**		6-311++G**		cc-pVDZ		cc-pVTZ	
parameter	pre	TS	pre	TS	pre	TS	pre	TS	pre	TS
$C_\alpha-C_\beta$	1.515	1.392	1.513	1.391	1.514	1.391	1.512	1.395	1.511	1.387
$C_\beta-H_\beta$	1.086	1.404	1.086	1.399	1.086	1.387	1.093	1.396	1.084	1.412
		(29.3)		(28.8)		(27.7)		(27.7)		(30.3)
$C_\beta-O_1$	3.137	2.552	3.133	2.550	3.137	2.550	3.135	2.556	3.125	2.556
$H_\beta-O_1$	2.794	1.204	2.793	1.206	2.801	1.218	2.775	1.212	2.788	1.198
$C_\alpha-S$	1.785	2.317	1.785	2.313	1.785	2.319	1.790	2.301	1.779	2.305
		(29.8)		(29.6)		(29.9)		(28.5)		(29.6)
$S-O_1$	1.451	1.534	1.445	1.529	1.446	1.530	1.467	1.551	1.439	1.522
$S-O_2$	1.451	1.467	1.445	1.462	1.446	1.463	1.467	1.481	1.439	1.454
$S-C_3$	1.774	1.782	1.772	1.782	1.773	1.782	1.777	1.785	1.767	1.778
$C_\alpha-C_\beta-H_\beta$	110.6	95.6	110.7	95.4	110.8	95.7	110.4	95.4	110.7	94.7
$C_\beta-H_\beta-O_1$	98.1	156.1	97.9	156.3	97.7	156.3	98.9	156.9	97.8	156.6
$C_\beta-C_\alpha-S$	109.6	98.7	109.7	98.7	109.9	98.6	109.2	99.0	109.7	99.1
$C_\alpha-S-O_1$	108.0	90.5	107.9	90.6	108.0	90.5	107.8	91.0	108.2	90.7
$C_\alpha-S-O_2$	108.0	114.0	107.9	115.1	108.0	113.7	107.8	114.3	108.2	113.7
$C_\alpha-S-C_3$	103.9	125.7	104.0	124.4	104.1	126.1	104.2	125.3	104.0	126.6
$S-C_\alpha-C_\beta-H_\beta$	−60.2	−4.2	−60.3	−4.4	−60.3	−4.5	−59.9	−4.2	−60.2	−4.6
$C_3-S-C_\alpha-C_\beta$	180.0	110.1	180.0	110.9	180.0	111.3	180.0	110.6	180.0	111.7
$O_1-S-C_\alpha-C_\beta$	65.7	7.2	65.6	7.6	65.5	7.5	65.6	6.9	65.5	7.5
$O_2-S-C_\alpha-C_\beta$	−65.7	−112.0	−65.6	−111.5	−65.5	−111.1	−65.6	−112.1	−65.5	−110.5

[a] Bond lengths are in angstroms and bond angles in degrees. Values in parentheses provide the degree of extension (in percent) of the $C_\beta-H_\beta$ and $C_\alpha-S$ bond lengths compared with the precursor.

Table 2. Main Geometrical Characteristics of the Sulfonyl Precursor (pre) and Transition State (TS) of Ethylene (MP2 Results)[a]

	6-31G**		6-311G**		6-311++G**		cc-pVDZ		cc-pVTZ	
parameter	pre	TS	pre	TS	pre	TS	pre	TS	pre	TS
$C_\alpha-C_\beta$	1.522	1.399	1.526	1.404	1.526	1.405	1.528	1.412	1.521	1.397
$C_\beta-H_\beta$	1.087	1.378	1.092	1.402	1.092	1.385	1.101	1.393	1.087	1.410
		(26.8)		(28.4)		(26.8)		(26.5)		(29.7)
$C_\beta-O_1$	3.155	2.557	3.147	2.553	3.156	2.555	3.155	2.565	3.133	2.563
$H_\beta-O_1$	2.799	1.235	2.797	1.209	2.811	1.228	2.781	1.227	2.780	1.210
$C_\alpha-S$	1.794	2.332	1.794	2.283	1.795	2.297	1.805	2.285	1.788	2.283
		(30.0)		(27.2)		(28.0)		(26.6)		(27.7)
$S-O_1$	1.471	1.560	1.458	1.547	1.462	1.550	1.482	1.574	1.455	1.545
$S-O_2$	1.471	1.488	1.458	1.475	1.462	1.478	1.482	1.496	1.455	1.470
$S-C_3$	1.785	1.794	1.784	1.793	1.785	1.794	1.795	1.805	1.778	1.792
$C_\alpha-C_\beta-H_\beta$	110.3	97.0	110.4	95.8	110.6	96.2	110.0	96.0	110.4	95.1
$C_\beta-H_\beta-O_1$	98.8	156.1	98.4	155.6	98.1	155.6	99.5	156.5	98.6	156.2
$C_\beta-C_\alpha-S$	109.5	97.8	109.3	98.7	109.6	98.4	108.6	98.7	108.9	99.2
$C_\alpha-S-O_1$	107.8	90.7	107.8	91.6	107.9	91.4	107.7	91.9	108.0	91.5
$C_\alpha-S-O_2$	107.8	113.5	107.8	114.8	107.9	113.8	107.7	114.1	108.0	112.6
$C_\alpha-S-C_3$	103.6	126.5	103.3	124.0	103.5	125.3	103.3	124.7	103.3	127.4
$S-C_\alpha-C_\beta-H_\beta$	−60.1	−4.9	−60.1	−5.2	−60.3	−5.2	−59.8	−5.0	−60.1	−5.7
$C_3-S-C_\alpha-C_\beta$	180.0	110.2	180.0	111.9	180.0	112.0	180.0	111.1	180.0	112.7
$O_1-S-C_\alpha-C_\beta$	66.0	8.5	66.1	9.1	65.8	9.0	66.1	8.3	65.8	9.3
$O_2-S-C_\alpha-C_\beta$	−66.0	−111.6	−66.1	−111.1	−65.8	−110.9	−66.1	−112.3	−65.8	−109.5

[a] Bond lengths are in angstroms and bond angles in degrees. Values in parentheses provide the degree of extension (in percent) of the $C_\beta-H_\beta$ and $C_\alpha-S$ bond lengths compared with the precursor.

overestimated, by 0.004−0.100 Å, in the reactant state. Hence, it appears that, compared with the MP2 level, the MPW1K approximation tends to slightly delay the proton transfer relative to the breaking of the $C_\alpha-S_\alpha$ bond.

Whatever the basis set and the correlation method employed, all structural results consistently indicate that in the transition state the $C_\beta-H_\beta$ and $C_\alpha-S$ bonds are both stretched by ∼28%, compared with the reactant state (Tables 1 and 2). It can thus be safely stated that the thermal conversion of the alkylsulfonyl precursor of ethylene follows a fully concerted mechanism.

The energy barrier of the E_i reaction is presented in Table 3. It is immediately apparent that successive improvements of the basis set have rather similar effects at all selected theoretical levels. Whatever the basis set, the energies obtained from single-point calculations on the MP2/6-311++G** optimized structures are almost identical to the MP2 energies obtained after full optimization, which fully justifies further considerations on the results of higher order [MP3, MP4SDQ, and CCSD(T)] single-point calculations. Diffuse functions have only a marginal impact. Upon inspection of Table 3, it appears that the standard 6-311G** basis is flexible enough to ensure an accuracy of ∼1−2 kcal/mol on the computed MPW1K and MP2 barrier heights, compared with the cc-pVTZ results. Extrapolation of the CCSD(T)/cc-pVDZ barrier height to the cc-pVTZ basis by comparison with the MPW1K and MP2 entries leads to a benchmark activation energy ($\Delta U^{\ddagger}$) of ∼54 kcal/mol. If one takes the CCSD(T) results as the standard of comparison, the DFT/MPW1K approach performs nearly as well as the MP2

Table 3. Internal Activation Energy ($\Delta U^{\ddagger}$ in Kilocalories per Mole) of the Internal Limination Reaction Leading to Ethylene Computed with Various Theoretical Methods and Basis Sets of Increasing Size

basis set	MPW1K[a]	HF[b]	MP2[b]	MP2[a]	MP2[c]	MP3[a]	MP4(SDQ)[a]	CCSD[a]	CCSD(T)[a]
6-31G**	55.2	70.4	56.6	56.6	56.6	60.1	59.0	59.2	55.6
6-311G**	53.8	68.6	54.1	54.2	54.1	57.7	56.8	57.0	53.1
6-311++G**	53.4	68.1	52.8	52.9	52.8	56.7	55.7	56.0	52.1
cc-pVDZ	49.4	64.7	48.8	48.9	48.9	52.6	51.7	51.9	48.0
cc-pVTZ	55.8	72.7	54.5	54.5	54.4				54[d]

[b] Results of single-point calculations on MP2/6-311++G** optimized structures. [a] Results of single-point calculations on MPW1K/6-311++G** optimized structures. [c] Results of full geometry optimizations. [d] Extrapolation of the CCSD(T)/cc-pVDZ barrier height to the cc-pVTZ basis by comparison with the MPW1K and MP2 entries.

Table 4. Internal Energy (ΔU in Kilocalories per Mole) Required for the Dissociation of the CH_3-S Bond in $CH_3-SO_2-CH_3$ Computed as Single-Point Calculations of Various Theoretical Methods and Basis Sets of Increasing Size on MP2/cc-pVTZ Optimized Structures

basis set	MPW1K	UHF	UMP2	UMP3	UMP4(SDQ)	UCCSD	UCCSD(T)
6-31G*	71.7	54.2	72.5	70.7	69.1	68.2	68.4
6-31G**	71.4	54.0	72.3	70.4	68.7	67.9	68.2
6-311G**	70.9	53.9	73.2	71.0	69.2	68.5	69.0
6-311++G**	69.5	52.4	72.0	70.0	68.0	67.3	67.8
cc-pVDZ	67.4	49.7	68.3	66.0	64.2	63.5	63.8
cc-pVTZ	71.0	53.4	77.1	73.9	71.9	71.1	71.9

approach, with the advantage of a much more reduced computational cost. With all basis sets, at the CC level, the impact of perturbative triple excitations is noticeable compared with the CCSD level. Notice that, upon comparison of the results of complete MP2 optimizations of the molecular structure and the results of MP2 single-point calculations on the MP2/6-311++G** and MPW1K/6-311++G** structures, the computed barriers are not very sensitive to details of the computed geometries.

The release of bond orders in the transition state leads, through changes in the zero-point energies, to a lowering of the energy barrier by 4.5 kcal/mol (MPW1K/6-311G** result). An activation enthalpy $\Delta H^{\ddagger}$ of ~49.3 kcal/mol (MPW1K/6-311G** level) is thus correspondingly found.

3.2. Radical C−S Bond Dissociation of Dimethylsulfonyl. To evaluate the accuracy of the MPW1K functional in describing radical dissociations (bond dissociation energies, BDE) of sulfone species, the quality of MPW!K results is first assessed by comparison against a known experimental value, namely, the dissociation energy of the $C_\alpha-S$ bond (Figure 5) in dimethylsulfonyl ($CH_3-SO_2-CH_3$),[40] and further benchmark theoretical data.

The dissociation energy (ΔH) obtained at the UMPW1K/6-311G** level (64.2 kcal/mol) compares rather favorably with the energy (68 kcal/mol)[40] reported experimentally, which has been derived from an Arrhenius plot of the rates of pyrolysis of alkyl sulfones. The former theoretical value accounts for a zero-point energy correction of −6.7 kcal/mol.

Table 4 presents the radical bond dissociation energies of the CH_3-S bond in $CH_3-SO_2-CH_3$, which has been calculated at the UHF, UMPn ($n = 2-4$), UCCSD, and UCCSD(T) levels using basis sets of increasing size. It can again be seen that successive improvements of the basis set have overall rather similar effects at all selected theoretical levels. Diffuse functions lead to a decrease of the dissociation energy by ~1 kcal/mol only, with respect to the values obtained with the 6-311G** basis set. The energy lowering in going from the cc-pVDZ to the cc-pVTZ basis set is practically the same (8 kcal/mol) at the MP2, MP3, MP4(SDQ), CCSD, and CCSD(T) levels. The UMP2 energy differences overestimate the UCCSD and UCCSD(T) results by ~4 kcal/mol. The UMPW1K calculations ensure overall an accuracy of ~2.5 kcal/mol in comparison with the CCSD(T) results. At the UHF level, the calculated reaction energies are much too low, ~14 kcal/mol, due to the neglect of electron correlation. Subtracting the UMPW1K/6-311G** zero-point energy correction of 6.7 kcal/mol from the UCCSD(T)/cc-pVTZ energy difference (ΔU) results in a benchmark bond dissociation enthalpy (ΔH) of 65.2 kcal/mol. The excellent agreement between the UMPW1K/6-311G**, UCCSD(T)/cc-pVTZ, and experimental results justifies also the use of the MPW1K/6-311G** level for further studies of radical dissociation reactions with large sulfonyl precursors.

As shall be seen, another important aspect of the radical dissociations of sulfonyl precursors pertains to the computation of entropy contributions to Gibbs free energies. For the test case of the homolytic dissociation of the $C_\alpha-S$ bond in the dimethylsulfonyl compound, an RRHO vibrational analysis of the reactant and products leads to entropy differences (ΔS) of +42.65 and +42.72 cal mol^{-1} K^{-1} at the MP2/6-311G** and MPW1K/6-311G** levels, respectively. Also, zero-point vibrational energies amount to a lowering of the reaction energy by 6.28 kcal/mol at the MP2/6-311G** level and by 6.71 kcal/mol at the MPW1K/6-311G** level. Hence, it appears that the MP1WK functional is also perfectly suited for describing the outcome of vibrational effects on radical dissociations of sulfonyl compounds.

4. Origin of sp^3 Defects in the Sulfonyl Precursor Route

4.1. Direct Internal Elimination (E_i) Reaction into *trans*-Stilbene. The most stable conformation of the sulfonyl precursor of stilbene is that with the leaving group ($-SO_2$-alkyl) in an *anti* configuration with respect to the phenyl group attached to C_β. Starting from the sulfonyl precursor in this configuration, the E_i elimination reaction can follow two possible pathways. Depending on the rotation direction of the substituents about the central $C_\alpha-C_\beta$ bond and of the two oxygens of the sulfonyl group about the $C_\alpha-S$ bond, two different eclipsed $O-S-C_\alpha-$

(40) Benson, S. W. *Chem. Rev.* **1978**, *78*, 23.

$C_\beta-H$ conformations can be reached, which, through an E_i elimination of a sulfinic acid (alkyl-SO_2H), lead either to the cis- or the trans-form (path A in Figure 1) of stilbene.

The E_i conversion reactions into *trans*- and *cis*-stilbene are characterized by activation energies ($\Delta U^{\ddagger}$ at the MPW1K/6-311G** level) of 48.8 and 51.9 kcal/mol, respectively. Compared with its sulfoxide counterpart,[21] the activation energy pertaining to the E_i reaction on a sulfonyl precursor is ~20 kcal/mol larger. Also, the MPW1K/6-311G** reaction energies (ΔU) characterizing the E_i conversion into *trans*- and *cis*-stilbene, 18.6 and 22.5 kcal/mol, respectively, are markedly endothermic, which reflects the highly unstable nature of the alkyl-SO_2H compound.

The zero-point vibrations lead to a lowering of the energy barrier by ~4.8 kcal/mol. The corresponding MPW1K/6-311G** activation enthalpies ($\Delta H^{\ddagger}$) toward *trans*- and *cis*-stilbene, 44.0 and 47.1 kcal/mol, respectively, are in line with the experimental activation enthalpies reported for methyl 2-phenylethyl sulfone (47.0 ± 1.8 kcal/mol),[19] a compound closely related to our sulfone precursor.

The apparent lowering of the activation barriers, by 2−4 kcal/mol, compared with the elimination to ethylene, can be essentially attributed to enhanced stabilization of the transition state by conjugation and resonance of the phenyl groups with the double bond in formation. The transition state pertaining to the trans-product is characterized by a practically planar five-membered ring (C_α, S, O, H, and C_β). On the other hand, the transition state leading to the cis-isomer has an $O-S-C_\alpha-C_\beta$ torsion angle of ~10°.

Variations in the electric charges of the atoms involved in reaction A (in Figure 1) are presented in Table 5, based on the Mulliken and Natural Population Analyses of one-electron densities, at the MPW1K/6-311G** level. As is immediately apparent from this table, both analyses consistently point to the same trends. The lack of evidence for an intermediate stable carbocation, as in a "pure" E_1 reaction, is overall verified from the atomic electric charges on the C_α and C_β atoms. Nonetheless, the $C_\alpha-S$ chemical bond is stretched to a greater extent (~32%) than the $C_\beta-H$ bond (~23%) in the transition state derived from the sulfonyl precursor of *trans*-stilbene, indicating, in comparison with the sulfoxide precursor,[21] a drift of the reaction from a fully internal rearrangement toward an E_1-like mechanism. Charge variations indicate correspondingly a substantial increase of the electron density on the S and C_β atoms during the reaction and, on the contrary, a lowering of the electron density on the C_α and H_β atoms.

4.2. Direct Radical Pathway. If an elimination of the radical type would occur with the alkylsulfonyl precursors of PPV, it would start with a homolytic cleavage of the $C_\alpha-S$ bond (path B in Figure 1), followed by a radical splitting of the $C_\beta-H$ bond or of the $C-S$ bond in the $C-SO_2$ radical. The final products of this direct radical reaction pathway can be a *trans*-stilbene segment, an alkyl derivative, and/or various cross-linked structures (Figure 2). Ethylene[41] and SO_2 can also be formed if the breakage of the $C_\alpha-S$ bond is followed by a splitting of the alkyl$-SO_2$ bond.

The bond dissociation energy (BDE) of the $C_\alpha-S$ bond in the sulfonyl precursor (path B in Figure 1) is calculated to be ~52.3 kcal/mol (UMPW1K/6-311G** result including a ΔZPE correction of −4.8 kcal/mol), in close agreement with the experimental value (56 kcal/mol) reported for the BDE of the $C_\alpha-S$ bond in the $CH_3(SO_2)$-benzyl compound.[39] Because the BDE is much larger than the activation enthalpy found for the E_i reaction (44.0 kcal/mol), a homolytic reaction appears at first sight unlikely to be very competitive. However, some caution is needed at this point because entropy effects are not yet accounted for.

Table 5. Atomic Electric Charges and Charge Variations (Δ) Derived from a Mulliken Population Analysis, and, in Parentheses, Natural Population Analysis at the MPW1K/6-311G** Level

step	atom	reactant state	transition state (TS)	Δ
step A in Figure 1	O	−0.53	−0.55	−0.02
		(−0.97)	(−0.92)	(+0.05)
	S	**+1.04**	**+0.88**	−0.16
		(+2.14)	**(+1.69)**	**(−0.45)**
	C_α	−0.40	−0.34	+0.06
		(−0.40)	(−0.11)	**(+0.29)**
	C_β	−0.21	−0.28	−0.07
		(−0.41)	(−0.53)	**(−0.12)**
	H_β	+0.19	+0.34	+0.15
		(+0.23)	(+0.43)	**(+0.20)**
step D in Figure 3	O	−0.56	−0.52	+0.04
		(−0.94)	(−0.86)	(+0.08)
	S	**+0.84**	**+0.66**	−0.18
		(+1.43)	**(+1.08)**	(−0.35)
	C_α	−0.42	−0.36	+0.06
		(−0.37)	(−0.17)	(+0.20)
	C_β	−0.22	−0.27	−0.05
		(−0.42)	(−0.50)	(−0.08)
	H_β	+0.18	+0.32	+0.14
		(+0.24)	(+0.41)	(+0.17)
E_i conversion of the sulfoxide precursor of *trans*-stilbene[21] [a]	O	−0.62	−0.54	+0.08
		(−0.98)	(−0.87)	(+0.11)
	S	**+0.71**	**+0.52**	−0.19
		(+1.20)	**(+0.88)**	(−0.34)
	C_α	−0.41	−0.41	0.00
		(−0.36)	(−0.19)	(+0.17)
	C_β	−0.21	−0.26	−0.05
		(−0.42)	(−0.51)	(−0.09)
	H_β	+0.18	+0.32	+0.14
		(+0.24)	(+0.40)	(+0.16)

[a] ϕ-CHS(O)R$-CH_2-\phi$.

4.3. Mixed Competitive Reaction Pathways. A third possible route starts with an E_i elimination via the alkyl chain (path C in Figure 1). Because in practice the conversion of an unsaturated precursor polymer chain takes place in condensed phases, it can be assumed that, while the viscosity of the medium, that is, the stiffness of the polymer matrix, increases while the reaction proceeds, the rotation of the phenyl rings into the eclipsed conformation, which occurs during the E_i reaction, becomes strongly impeded by environmental effects. On the contrary, the flexibility of alkyl chains should remain practically unaffected. The question therefore arises whether matrix effects could easily overcome the differences in activation and reaction energies between an E_i reaction via the alkyl chain or the polymer backbone.

This competive E_i pathway via the alkyl chain (path C in Figure 1) requires an activation enthalpy ($\Delta H^{\ddagger}$) of 48.8 kcal/mol (MPW1K/6-311G** result). The corresponding reaction energy (ΔU) is ~ +28.8 kcal/mol. The activation enthalpy is only slightly higher than that associated with the E_i reaction (44.0 kcal/mol) via the polymer backbone (path A in Figure 1). It is, on the other hand, slightly lower than the energy

(41) Octene, when considering an *n*-octylsulfonyl precursor. See remark on precursors in the Introduction.

Table 6. Temperature Dependence of Thermodynamical Quantities for the E_i and Radical Pathways of Figure 1 (MPW1K/6-311G** Results, in Kilocalories per Mole)

	step A in Figure 1			step B in Figure 1			step C in Figure 1		
T (K)	$\Delta H^{\ddagger}$ (T)	$T\Delta S^{\ddagger}$ (T)	$\Delta G^{\ddagger}$ (T)	ΔH (T)	$T\Delta S$ (T)	ΔG (T)	$\Delta H^{\ddagger}$ (T)	$T\Delta S^{\ddagger}$ (T)	$\Delta G^{\ddagger}$ (T)
298	44.2	0.2	44.0	52.9	15.5	37.4	48.7	0.1	48.5
325	44.2	0.2	44.0	52.9	16.9	36.0	48.7	0.1	48.5
350	44.2	0.2	44.0	52.9	18.2	34.7	48.7	0.2	48.5
375	44.2	0.3	43.9	52.9	19.5	33.4	48.7	0.2	48.5
400	44.2	0.3	43.9	52.9	20.8	32.1	48.7	0.2	48.5
450	44.2	0.4	43.9	52.9	23.3	29.5	48.7	0.3	48.5
500	44.3	0.4	43.8	52.8	25.9	27.0	48.8	0.3	48.4
550	44.3	0.5	43.8	52.7	28.4	24.4	48.8	0.4	48.4
600	44.3	0.5	43.8	52.7	30.9	21.8	48.8	0.4	48.4

required (BDE = 52.3 kcal/mol) for a radical dissociation of the $C_\alpha-S$ bond (path B in Figure 1). As a difference of activation energies of ~5 kcal/mol can be easily compensated for by environmental effects, due to the reduced conformational freedom of conjugated segments in a polymer matrix, E_i reactions via the alkyl chain are very likely to be competitive. After elimination through this reaction channel, ethylene[41] is formed. The produced sulfinic acid (**2**) can be converted into *trans*-stilbene via an E_i reaction (path D in Figure 3) or a radical cleavage of the $C_\alpha-S$ bond (path E in Figure 3), which can lead again to *trans*-stilbene, alkyl derivatives, or cross-linked structures via side and cross-linked reactions.

The activation enthalpy ($\Delta H^{\ddagger}$) of the "second" E_i elimination (reaction D in Figure 3) is found to be 27.2 kcal/mol, whereas for the radical mechanism (reaction E in Figure 3) a BDE of 37.9 kcal/mol is required. Here also, the E_i path appears therefore to be enthalpically favored. However, as an activation barrier of 48.8 kcal/mol had already to be overcome (path C in Figure 1), implying in practice rather high temperatures (550 K), and because the subsequent reactions in Figure 3 require lower activation energies, it can already be concluded that these reactions will certainly not be very selective.

Note also that the energy barrier characterizing the E_i conversion of the sulfinic acid (**2**) in *trans*-stibene (reaction D in Figure 3) is ~17 kcal/mol lower than that of the E_i conversion of the sulfonyl precursor (path A in Figure 1), but ~3 kcal/mol higher than that for the E_i conversion of a sulfoxide precursor[21] ($\Delta H^{\ddagger}$ = 24.9 kcal/mol). These variations in the energy barrier can be directly related to changes in the oxidation state of the sulfur atom in these compounds, which is best quantified by the extent of the positive electric charge on this atom (Table 5).

Both Mulliken and NPA charges (Table 5) point out a strong electron withdrawal for the sulfur atom from the reactant state to the transition state. As can be expected for a reaction involving considerable charge transfers, the activation barrier is lowered with the decreasing polarity of the $C_\alpha-S$ bond. Stronger similarities can be noticed between the distributions of charges in the sulfinic acid (**2**) and the sulfoxide precursor of *trans*-stilbene.[21] In line with this observation, the E_i reaction of the intermediate **2** (path D in Figure 3) resembles from its activation enthalpy ($\Delta H^{\ddagger}$ = 27.2 kcal/mol) more the E_i reaction of the sulfoxide precursor ($\Delta H^{\ddagger}$ = 24.9 kcal/mol) than that of a sulfonyl precursor (A in Figure 1, $\Delta H^{\ddagger}$ = 44.0 kcal/mol). Notice that the energy required for the radical breaking of the $C_\alpha-S$ bond in the sulfinic acid **2** (path E in Figure 3) is ~14 kcal/mol lower than that required for the breaking of the $C_\alpha-S$ bond of the original sulfonyl precursor (path B in Figure 1). Hence, E_i conversion through the alkyl chain would be straightforwardly allowed by numerous radical reactions leading to sp^3 defects.

After the homolytic cleavage of the $C_\alpha-S$ bond (path E in Figure 3), SO_2 can be eliminated from the O═S—OH radical, leaving behind a hydrogen radical that can, for instance, react with ethylene[41] to form alkyl radicals. Depending on the recombination of the radicals, sp^3 defects or cross-linked structures can be formed (path E in Figure 3). This alternative path also provides a consistent explanation to the experimentally observed restricted conjugation length and structural defects in the obtained PPV polymer.[16]

4.4. Entropy Effects and Thermal Corrections. Entropy effects have been included in the calculations to allow for a direct comparison with experiment. Temperatures ranging from 300 to 600 K have been considered.

For the E_i conversions of the sulfonyl precursors (reactions A and C in Figure 1) the activation enthalpies [$\Delta H^{\ddagger}$ (T)] only increase by 0.1 kcal/mol over the considered temperature range, whereas (Table 6) a slight decrease by 0.3 kcal/mol is observed for the competitive radical pathway (reaction B in Figure 1). Similarly, the entropy contribution $T\Delta S^{\ddagger}$ (T) to the Gibbs free activation energies is very limited for the E_i reactions A and C in Figure 1, even at temperatures as high as 600 K (Table 6). On the contrary, for the radical bond dissociation reaction of the sulfonyl precursor of *trans*-stilbene, the entropy contributions to the Gibbs free reaction energy are found to grow significantly with increasing temperature (Table 6). In particular, entropy effects amount to a lowering of ΔG ranging from 15 kcal/mol at 300 K to 31 kcal/mol at 600 K. Therefore, upon comparison of the Gibbs free activation energies of the possible reaction routes toward *trans*-stilbene, it is clear that the direct radical pathway will therefore be entropically strongly favored over the E_i pathways at the range of temperatures (500−600 K) usually imposed to perform the conversion. Notice that radical reactions will be also further favored in a rigid polymer matrix, because the sterical requirements of such reactions are much less than with E_i conversions.

Also, it should be noted that the difference in Gibbs free activation energy for pathways A and C is only 4.5 kcal/mol. In a sterically strained environment such as a polymer matrix, the energy difference between paths A and C can be easily accommodated by the relatively easy rotation of the alkyl chain in comparison with the more limited conformational freedom of an extended polymer backbone. Similarly, when the temperature is increased from 300 to 600 K, a small decrease is observed for the activation entropies [$\Delta S^{\ddagger}$ (T)] characterizing the E_i conversion of intermediate **2** (reaction D in Figure 3), whereas a significant increase is again calculated for the reaction

Table 7. Temperature Dependence of Thermodynamical Quantities for the E_i and Radical Pathways in a Vacuum in Figure 3 (MPW1K/6-311G** Results, in Kilocalories per Mole)

	step D in Figure 3			step E in Figure 3		
T (K)	$\Delta H^{\ddagger}$ (T)	$T\Delta S^{\ddagger}$ (T)	$\Delta G^{\ddagger}$ (T)	ΔH (T)	$T\Delta S$ (T)	ΔG (T)
298	27.1	−0.8	27.9	38.3	14.8	23.6
325	27.1	−0.9	28.0	38.3	16.0	22.2
350	27.1	−0.9	28.0	38.2	17.2	21.0
375	27.1	−1.0	28.1	38.2	18.4	19.8
400	27.1	−1.1	28.2	38.1	19.6	18.5
450	27.1	−1.2	28.3	38.0	21.9	16.1
500	27.0	−1.4	28.4	37.8	24.1	13.7
550	27.0	−1.6	28.6	37.6	26.3	11.3
600	27.0	−1.7	28.7	37.4	28.5	8.9

Table 8. Detailed Analysis of the Activation Entropies Characterizing at Various Temperatures the Internal Elimination Pathways (A, C, and D) of Figures 1 and 3 (Results in Calories per Mole per Degree Kelvin)[a]

T (K)		step A	step C	step D
298	$\Delta S^{\mathrm{rot.}\ddagger}$	0.28	0.11	0.16
	$\Delta S^{\mathrm{vib}\ddagger}$	0.29	0.32	−2.77
	$\Delta S^{\mathrm{total}\ddagger}$	0.56	0.43	−2.61
400	$\Delta S^{\mathrm{rot.}\ddagger}$	0.27	0.11	0.16
	$\Delta S^{\mathrm{vib}\ddagger}$	0.45	0.41	−2.87
	$\Delta S^{\mathrm{total}\ddagger}$	0.73	0.51	−2.71
500	$\Delta S^{\mathrm{rot.}\ddagger}$	0.27	0.11	0.16
	$\Delta S^{\mathrm{vib}\ddagger}$	0.55	0.51	−2.95
	$\Delta S^{\mathrm{total}\ddagger}$	0.83	0.62	−2.79
600	$\Delta S^{\mathrm{rot.}\ddagger}$	0.27	0.11	0.16
	$\Delta S^{\mathrm{vib}\ddagger}$	0.61	0.60	−3.00
	$\Delta S^{\mathrm{total}\ddagger}$	0.88	0.71	−2.85

[a] $\Delta S^{\mathrm{trans}\ddagger} = \Delta S^{\mathrm{elec}\ddagger} = 0$.

entropy pertaining to the competitive radical pathway (step E in Figure 3; Table 7). In turn, at high temperatures, path E could therefore also lead to numerous sp^3 defects in the final material.

The activation or reaction entropies for the five reactions (A−E) investigated in the present study are analyzed in detail in Tables 8 and 9. Only the rotational and vibrational components contribute in a nonvanishing way to the activation entropy of the internal elimination reactions (Table 8). For such reactions, both contributions remain small, whatever the temperature. One remarkable feature emerging from Table 8 is that the rotational contribution to the activation entropy of the E_i reactions remains practically constant upon an increase of the temperature. In sharp contrast, the dominant contribution to the reaction entropy of the radical dissociations (Table 9) arises from translation and is seen to rapidly increase with increasing temperatures. In this case, translations and rotations both lead to substantial positive contributions to the reaction entropy, whereas the contribution arising from vibrations is smaller and negative. These significant variations in the rotational, vibrational, and translational components of the entropies simply relate to the fact that, because of the homolytic cleavage of the precursor into two molecular fragments, three additional rotational and three additional translational degrees of freedom are becoming available, at the expense of six internal (vibrational) degrees of freedom. In the RRHO depiction, at temperatures between 300 and 600 K, the rotational entropy of the largest fragment (ϕ-CH$^{\bullet}$−CH$_2$-ϕ) is only ∼1.5 cal mol^{-1} K^{-1} lower than that of the original sulfonyl (**1**) or sulfinic acid (**2**) precursor; hence, the increase in rotational entropy mostly arises

Table 9. Detailed Analysis of the Reaction Entropies Characterizing at Various Temperatures the Radical Dissociation Pathways (B and E) of Figures 1 and 3 (Results in Calories per Mole per Degree Kelvin)

T (K)		step B	step E
298	$\Delta S^{\mathrm{trans}}$	37.9	37.5
	ΔS^{elec}	2.8	2.8
	$\Delta S^{\mathrm{rot.}}$	22.9	21.0
	ΔS^{vib}	−11.6	−11.7
	$\Delta S^{\mathrm{total}}$	52.0	49.6
400	$\Delta S^{\mathrm{trans}}$	39.4	39.0
	ΔS^{elec}	2.8	2.8
	$\Delta S^{\mathrm{rot.}}$	23.8	21.9
	ΔS^{vib}	−14.0	−14.7
	$\Delta S^{\mathrm{total}}$	51.9	48.9
500	$\Delta S^{\mathrm{trans}}$	40.5	40.1
	ΔS^{elec}	2.8	2.8
	$\Delta S^{\mathrm{rot.}}$	24.5	22.6
	ΔS^{vib}	−16.0	−17.2
	$\Delta S^{\mathrm{total}}$	51.7	48.2
600	$\Delta S^{\mathrm{trans}}$	41.4	41.0
	ΔS^{elec}	2.8	2.8
	$\Delta S^{\mathrm{rot.}}$	25.0	23.1
	ΔS^{vib}	−17.7	−19.3
	$\Delta S^{\mathrm{total}}$	51.5	47.6

because of the detachment of a small alkyl−$SO_2^{\bullet}$ or H−$SO_2^{\bullet}$ particle. The breaking of a singlet closed-shell species into two open-shell doublet fragments results also in a minor electronic contribution to the reaction entropy of the radical dissociations (Table 9).

5. Conclusions and Outlook for the Future

In the present study, quantum-chemical calculations have been carried out to identify on reliable grounds the origin of the structural defects observed in samples of poly(*p*-phenylene vinylene) (PPV) prepared by thermal conversion of alkylsulfonyl precursors. Three major reaction pathways have been identified in the process and investigated in the present study: a direct E_i conversion via the polymer backbone, a conversion via a radical dissociation of the precursor, and a mixed pathway starting with an E_i reaction via the alkyl chain, followed by side reactions involving further radical dissociation of the obtained intermediate. This study focuses, above all, on a quantitative determination of the activation or reaction enthalpies characterizing these reactions in the vacuum, by means of the MPW1K functional, and provides in addition more qualitative insights into entropy effects, at the level of the standard RRHO approximation. In a preliminary step, the performance of the MPW1K functional in describing the internal elimination and radical dissociations of sulfonyl precursors has been assessed by comparison with the results of a variety of calculations, up to the benchmark CCSD(T) level, on the sulfonyl precursor of ethylene and on dimethylsulfonyl, respectively. The E_i reactions via the polymer backbone and the alkyl chain are enthalpically easier than the radical dissociations. Conversely, at the relatively high temperatures under which the conversion is performed, entropy effects tend to favor the radical dissociations over the internal elimination reactions, a fact that has been largely overlooked so far in studies of the chemical reactivity of sulfonyl precursors.

In the present work, we did not consider complications such as centrifugal distortions of the rotating molecules, couplings of the external rotations with hindered internal rotations via

Coriolis forces, couplings between rotations and vibrations, and vibrational anharmonicities. Further highly demanding investigations, beyond the RRHO approximation and the current computational possibilities, would be necessary to quantitatively clarify the outcome of such effects on the computed activation and reaction entropies. However, because the most important contributions to the activation entropies of radical dissociations are obviously due to translations, there is no reason to think that, even at temperatures as high as 600 K [RT $\sim$ 1.2 kcal mol^{-1}], the above deficiencies of the RRHO model could qualitatively call into question the trends emerging from our calculations (in the investigated compounds, the lowest rotational barriers amount to $\sim$2.5 kcal mol^{-1}). It has in particular been found that entropy contributions very strongly lower the Gibbs free reaction energies pertaining to radical dissociations, whereas the entropy contribution to the Gibbs free energy barrier describing internal elimination reactions is quasi-insignificant. Such a sharp difference relates to the very simple fact that, with any bond cleavage, six vibrational degrees of freedom are converted into three rotational and three translational degrees of freedom.

From the present results it can therefore be safely concluded that a radical pathway, starting with a homolytic breakage of the $C_\alpha-S$ bond of the sulfonyl group, represents one of the most important channels at the origin of sp^3 structural defects in PPV materials prepared by a thermal conversion at high temperatures of sulfonyl precursor chains. Further indirect pathways that will also significantly contribute to the formation of such defects imply competitive E_i conversions of the precursor through the external alkyl substituent rather than through the central $C_\alpha-C_\beta$ segment, prior to entropically strongly favored radical dissociations of the produced sulfinic acid intermediates. Temperature will therefore be one of the most important parameters to control for a fine-tuning of the average conjugation length and, thus, electro-optical properties of conjugated polymers synthesized via the sulfonyl precursor route.

Acknowledgment. L.C. acknowledges a Ph.D. grant from the Bijzonder Onderzoeksfonds (BOF) of the Limburgs Universitair Centrum, within the framework of a multidisciplinary project on "Conjugated Organic Polymers for Polymer Electronics" (COPPEC). M.S.D. thanks the Fonds voor Wetenschappelijk Onderzoek (FWO) van Vlaanderen, the Flemish branch of the National Science Foundation in Belgium, for financial support. We are grateful to Els Kesters and Profs. Dirk Vanderzande and Jan Gelan (Research Group Organic and Polymer Chemistry, LUC, Belgium) for useful discussions and support.

JA021295E